Electronic Supplementary Material (ESI) for Journal of Materials Chemistry C.
This journal is © The Royal Society of Chemistry 2020

Electronic Supplementary Information (ESI)

Universal Polymeric Bipolar Hosts for Highly Efficient Solution-Processable Blue and Green Thermally Activated Delayed Fluorescence OLEDs

Jinhyo Hwang,[§] Chae Yeong Kim,[§] Hyunchul Kang, Ji-Eun Jeong, Han Young Woo, Min Ju Cho,* Sungnam Park, and Dong Hoon Choi*

Department of Chemistry, Research Institute for Natural Sciences, Korea University, 145 Anam-ro, Seongbuk-gu, Seoul, 02841, Republic of Korea.

*Corresponding authors: chominju@korea.ac.kr, dhchoi8803@korea.ac.kr

[§]These authors contributed equally to this work.

Experimental Section

Instrumentation

^{1}H and ^{13}C nuclear magnetic resonance (NMR) spectra were recorded using Varian Mercury 500-MHz spectrometers in $CDCl_3$ solvent. Mass spectrometry was performed using Bruker Daltonics. DSC (DSC, Mettler 821 Instrument) and TGA using a TGA Q500 V20.13 build 39 were performed to investigate the thermal properties of the host materials.

Absorption spectra of the host materials were measured using a UV-vis absorption spectrophotometer (HP 8453, λ = 190–1100 nm). PL spectra were also recorded at room temperature (298 K) and at low temperature (77 K) (Hitachi F-7000 and Thermo FA-357 fluorescence spectrophotometer). Triplet energies were obtained from the onset wavelength of the low-temperature PL spectra measured at 77 K. To measure the oxidation potential of the host in the film state, cyclic voltammetry was performed at a scanning rate of 50 mV s^{-1} using a potentiostat (EA161, eDAQ).

Theoretical Calculations

We used the commercially available Gaussian 16 software package to optimize the simplified molecular structure of **P(NmCP)** and **P(mCP)**, frontier molecular orbitals (HOMO and LUMO), and excitation states (S_1 and T_1 states) based on the B3LYP function and 6-31G *.

Single carrier devices

The construction and analysis of single carrier devices such as HODs and EODs using **P(NmCP)** and **P(mCP)** host materials were performed according to a previously published method.[1,2] HODs and EODs with a multilayered device structure were composed of ITO/PEDOT: PSS (40

nm)/PX2Cz (20 nm)/Host (15 nm)/Al (100 nm) and ITO/Host (15 nm)/TPBi (40 nm)/LiF (0.8 nm)/Al(100 nm).

Sky-blue and Green TADF-OLED Fabrication and Characterization

The sky-blue and green TADF device structures comprised ITO/PEDOT: PSS (40 nm)/PX2Cz(20 nm)/ Host: 5CzCN (15 nm, 5, 10, 20, and 30 wt.%) or t4CzIPN (15 nm, 3, 6, and 9 wt.%)/TPBi (40 nm)/LiF (0.8 nm)/Al (100 nm). Prior to device fabrication, the ITO-coated substrates were washed according to the procedure previously described in the literature.[2] PEDOT:PSS (40 nm) was deposited on the ITO-coated substrates at a spin rate of 4000 rpm for 40 s and then annealed at 155 °C for 15 min. The 0.5 wt.% PX2Cz solution was prepared from a chlorobenzene solvent, spin-coated on top of the ITO/PEDOT:PSS, and subsequently annealed at 100 °C for 60 s under UV illumination. The emitting layers were prepared from a toluene solution and spin-coated at 3000 rpm for 30 s. TPBi with a thickness of 40 nm was deposited under high vacuum conditions. Finally, LiF and Al electrodes were produced by vacuum deposition. The characteristics of the OLED device were measured using a Keithley SMU 236 instrument and a SpectraScan PR-655 colorimeter.

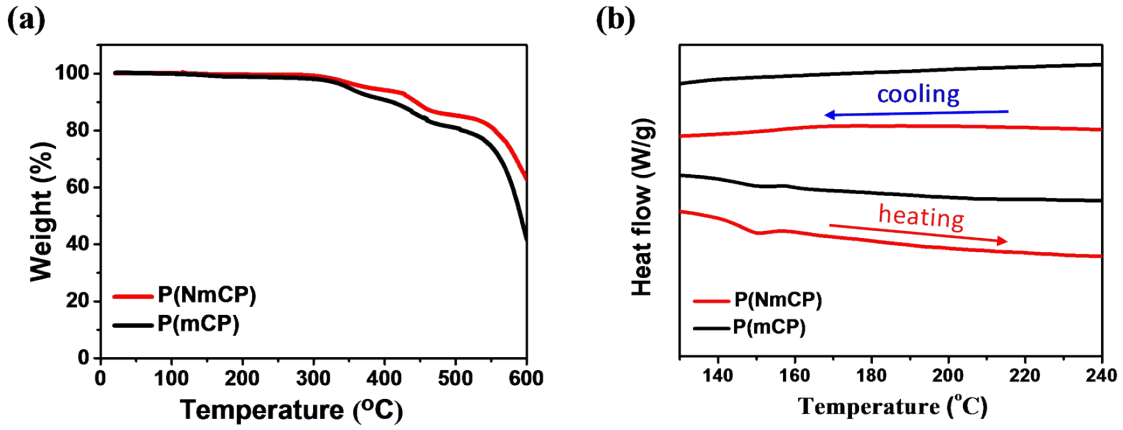

Figure S1. (a) TGA thermograms recorded at a heating rate of 10 °C/min under nitrogen atmosphere and (b) DSC traces recorded at a heating rate of 10 °C/min under nitrogen atmosphere.

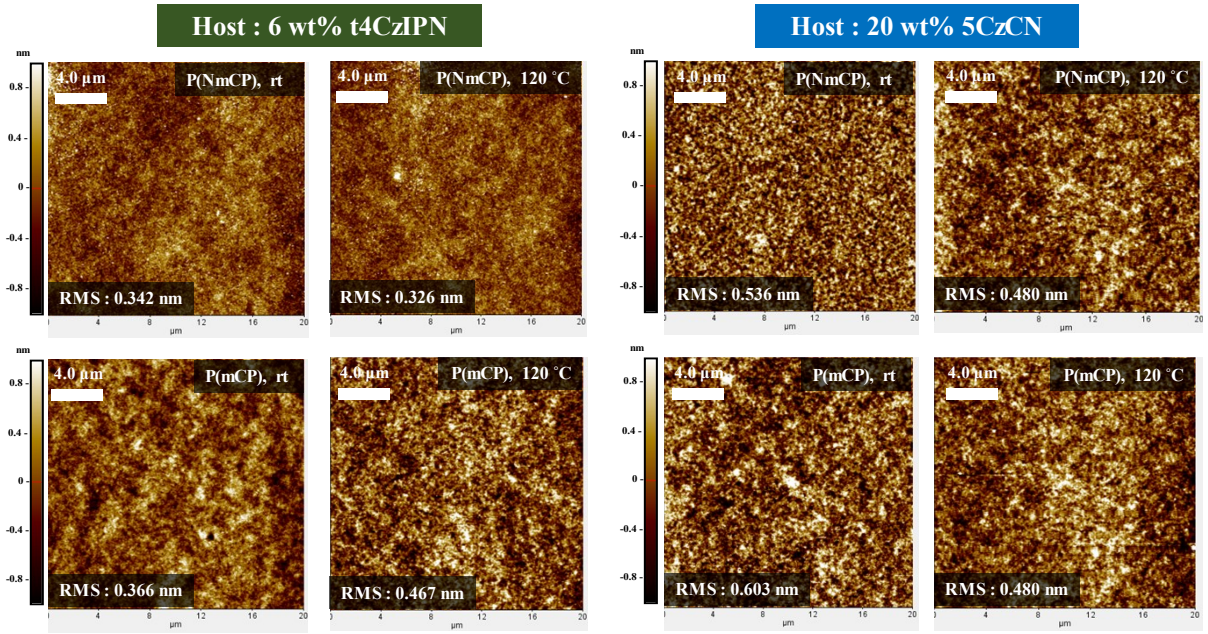

Figure S2. AFM height images of the blend films with the polymer host and dopants before and after thermal annealing at 120°C.

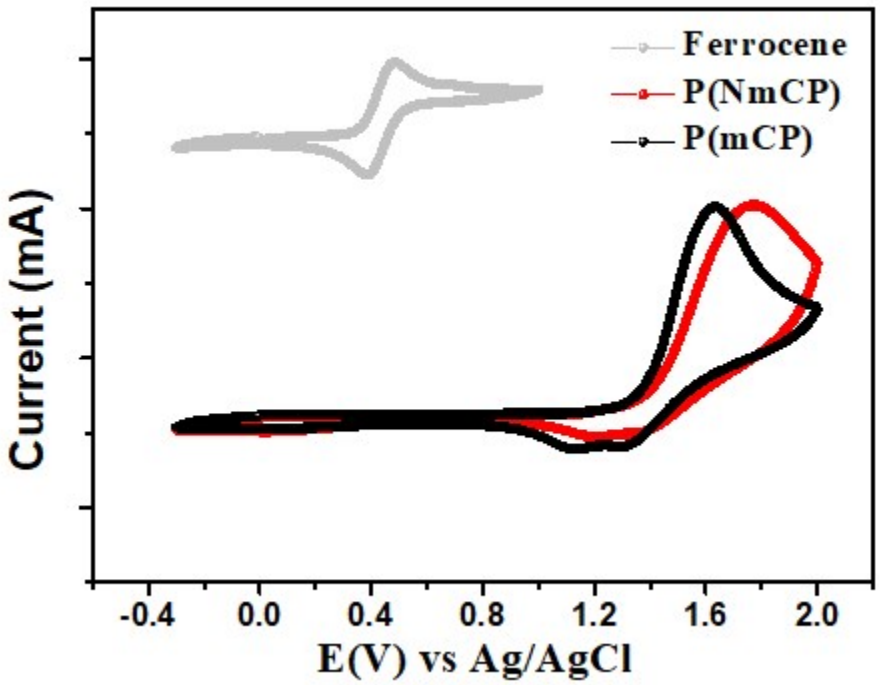

Figure S3. Cyclic voltammograms of **P(mCP)** and **P(NmCP)** in film states.

Determination of all rate constants associated with thermally activated delayed fluorescence kinetics of a dopant with a relatively small PLQY[1]

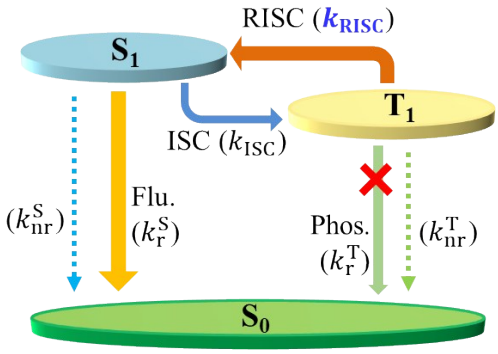

The TADF kinetics associated with the lowest singlet excited state (S_1), triplet excited state (T_1), and singlet ground state (S_0) can be described as shown in the above figure. The coupled differential equations for the populations of the S_1 and T_1 states are written as

$$\frac{d[\mathrm{S_1}]}{dt} = -(k_{\mathrm{r}}^{\mathrm{S}} + k_{\mathrm{nr}}^{\mathrm{S}} + k_{\mathrm{ISC}})[\mathrm{S_1}] + k_{\mathrm{RISC}}[\mathrm{S_1}]$$

$$\frac{d[\mathrm{T_1}]}{dt} = k_{\mathrm{ISC}}[\mathrm{S_1}] - (k_{\mathrm{nr}}^{\mathrm{T}} + k_{\mathrm{RISC}})[\mathrm{T_1}]$$

where $k_{\mathrm{r}}^{\mathrm{S}}$ is the rate constant for radiative decay from the first singlet excited state (S_1); k_{ISC} and k_{RISC} depict the rate constants for the intersystem crossing (ISC) and RISC between the S_1 and T_1 states, respectively; and $k_{\mathrm{nr}}^{\mathrm{T}}$ and $k_{\mathrm{nr}}^{\mathrm{S}}$ represent the rate constants for non-radiative decay from the T_1 and S_1 states, respectively. Upon solving the above coupled differential equations for $[\mathrm{S_1}]$, the following equation should be reached:

$$[\mathrm{S_1}] = A_{\mathrm{PF}} \exp(-k_{\mathrm{PF}}t) + A_{\mathrm{DF}} \exp(-k_{\mathrm{DF}}t)\,,\ A_{\mathrm{PF}} + A_{\mathrm{DF}} = 1$$

$$k_{\mathrm{PF}}, k_{\mathrm{DF}} = \frac{k_{\mathrm{r}}^{\mathrm{S}} + k_{\mathrm{nr}}^{\mathrm{S}} + k_{\mathrm{ISC}} + k_{\mathrm{nr}}^{\mathrm{T}} + k_{\mathrm{RISC}}}{2} \times \left(1 \pm \sqrt{1 - \frac{4(k_{\mathrm{r}}^{\mathrm{S}} + k_{\mathrm{nr}}^{\mathrm{S}} + k_{\mathrm{ISC}})(k_{\mathrm{nr}}^{\mathrm{T}} + k_{\mathrm{RISC}}) - 4k_{\mathrm{ISC}}k_{\mathrm{RISC}}}{(k_{\mathrm{r}}^{\mathrm{S}} + k_{\mathrm{nr}}^{\mathrm{S}} + k_{\mathrm{ISC}} + k_{\mathrm{nr}}^{\mathrm{T}} + k_{\mathrm{RISC}})^2}}\right)$$

Because the rate constants associated with the singlet excited state are significantly larger than those associated with the triplet excited state (i.e., $k_{\mathrm{r}}^{\mathrm{S}}, k_{\mathrm{nr}}^{\mathrm{S}}, k_{\mathrm{ISC}} \gg k_{\mathrm{nr}}^{\mathrm{T}}, k_{\mathrm{RISC}}$), k_{PF} and k_{DF} are approximately written as:

$$k_{\mathrm{PF}} = k_{\mathrm{r}}^{\mathrm{S}} + k_{\mathrm{nr}}^{\mathrm{S}} + k_{\mathrm{ISC}}$$

$$k_{\mathrm{DF}} = k_{\mathrm{nr}}^{\mathrm{T}} + \left(1 - \frac{k_{\mathrm{ISC}}}{k_{\mathrm{r}}^{\mathrm{S}} + k_{\mathrm{nr}}^{\mathrm{S}} + k_{\mathrm{ISC}}}\right) k_{\mathrm{RISC}} = k_{\mathrm{nr}}^{\mathrm{T}} + \left(1 - \frac{k_{\mathrm{ISC}}}{k_{\mathrm{PF}}}\right) k_{\mathrm{RISC}}$$

The quantum efficiencies of the prompt fluorescence (PF) and delayed fluorescence (DF) are given by

$$\Phi_{\mathrm{PF}} = \frac{k_{\mathrm{r}}^{\mathrm{S}}}{k_{\mathrm{r}}^{\mathrm{S}} + k_{\mathrm{nr}}^{\mathrm{S}} + k_{\mathrm{ISC}}} = \frac{k_{\mathrm{r}}^{\mathrm{S}}}{k_{\mathrm{PF}}}$$

$$\Phi_{\mathrm{DF}} = \sum_{k=1}^{\infty} \left(\Phi_{\mathrm{ISC}}\Phi_{\mathrm{RISC}}\right)^{k} \Phi_{\mathrm{PF}} = \frac{\Phi_{\mathrm{ISC}}\Phi_{\mathrm{RISC}}}{1-\Phi_{\mathrm{ISC}}\Phi_{\mathrm{RISC}}}\Phi_{\mathrm{PF}}$$

where Φ_{PF} and Φ_{DF} are the quantum yields for the PF and DF, respectively. The quantum efficiencies for the non-radiative relaxation, ISC, and RISC, are given by

$$\Phi_{\mathrm{nr}}^{\mathrm{S}} = \frac{k_{\mathrm{nr}}^{\mathrm{S}}}{k_{\mathrm{r}}^{\mathrm{S}} + k_{\mathrm{nr}}^{\mathrm{S}} + k_{\mathrm{ISC}}} = \frac{k_{\mathrm{nr}}^{\mathrm{S}}}{k_{\mathrm{PF}}}$$

$$\Phi_{\mathrm{ISC}} = \frac{k_{\mathrm{ISC}}}{k_{\mathrm{r}}^{\mathrm{S}} + k_{\mathrm{nr}}^{\mathrm{S}} + k_{\mathrm{ISC}}} = \frac{k_{\mathrm{ISC}}}{k_{\mathrm{PF}}}$$

$$\Phi_{\mathrm{RISC}} = \frac{k_{\mathrm{RISC}}}{k_{\mathrm{nr}}^{\mathrm{T}} + k_{\mathrm{RISC}}}$$

When the non-radiative relaxation of the triplet state ($k_{\mathrm{nr}}^{\mathrm{T}}$) is significantly slower than that of k_{RISC} (i.e., $k_{\mathrm{RISC}} \gg k_{\mathrm{nr}}^{\mathrm{T}}$), $\Phi_{\mathrm{RISC}} = \frac{k_{\mathrm{RISC}}}{k_{\mathrm{nr}}^{\mathrm{T}} + k_{\mathrm{RISC}}} \simeq 1$ and $\Phi_{\mathrm{DF}} \simeq \frac{\Phi_{\mathrm{ISC}}}{1-\Phi_{\mathrm{ISC}}}\Phi_{\mathrm{PF}}$. The quantum efficiency for the ISC is approximately obtained by $\Phi_{\mathrm{ISC}} \simeq \frac{\Phi_{\mathrm{DF}}}{\Phi_{\mathrm{PF}} + \Phi_{\mathrm{DF}}}$, where Φ_{PF} and Φ_{DF} are the quantum yields for the PF and DF, respectively. Therefore, when k_{PF}, k_{DF}, $\Phi_{\mathrm{PF}} = A_{\mathrm{PF}}\Phi_{\mathrm{PL}}$, and $\Phi_{\mathrm{DF}} = A_{\mathrm{DF}}\Phi_{\mathrm{PL}}$ (Φ_{PL}, PLQY) are experimentally determined by measuring the time-dependent PL signal, $[\mathrm{S}_1] = A_{\mathrm{PF}}\exp(-k_{\mathrm{PF}}t) + A_{\mathrm{DF}}\exp(-k_{\mathrm{DF}}t)$ and $A_{\mathrm{PF}} + A_{\mathrm{DF}} = 1$, the rate constants associated with the TADF kinetics of a dopant in host films, are readily estimated as

$$k_{\mathrm{r}}^{\mathrm{S}} = k_{\mathrm{PF}}\Phi_{\mathrm{PF}}$$

$$k_{\mathrm{ISC}} \simeq k_{\mathrm{PF}} \frac{\Phi_{\mathrm{DF}}}{\Phi_{\mathrm{PF}} + \Phi_{\mathrm{DF}}}$$

$$k_{\mathrm{nr}}^{\mathrm{S}} \simeq k_{\mathrm{PF}} \left(1 - \Phi_{\mathrm{PF}} - \frac{\Phi_{\mathrm{DF}}}{\Phi_{\mathrm{PF}} + \Phi_{\mathrm{DF}}} \right)$$

$$k_{\mathrm{RISC}} = \frac{k_{\mathrm{PF}} \cdot k_{\mathrm{DF}}}{k_{\mathrm{ISC}}} \cdot \frac{\Phi_{\mathrm{DF}}}{\Phi_{\mathrm{PF}}}$$

The kinetic model here may be useful to describe the photophysical behavior of a dopant, in which the non-radiative relaxation mostly occurs from the singlet excited state (S_1), and the PLQY (Φ_{PL}) is dictated mostly by $k_{\mathrm{nr}}^{\mathrm{S}}$. The dopant molecules (5CzCN and t4CzIPN) used in this study exhibited relatively small PLQY (Φ_{PL} , 63%–66%), which deviated significantly from 100%. It can be readily assumed that the non-radiative relaxation from the S_1 state ($k_{\mathrm{nr}}^{\mathrm{S}}$) was responsible for the low PLQY.

Table S1. Photophysical properties and kinetic parameters of doped films.

Host	Dopant	τ_p (ns) [a]	τ_d (μs) [b]	Φ_{PL} (%) [c]	Φ_p (%) [d]	Φ_d (%) [e]	k_r^S (10^7 s^{-1}) [f]	k_{nr}^S (10^7 s^{-1}) [g]	k_{ISC} (10^7 s^{-1}) [h]	k_{RISC} (10^7 s^{-1}) [i]
P(NmCP)	5CzCN (20 wt.%)	19.88	6.07	69.2	11.40	57.80	0.57	0.25	0.42	0.099
P(mCP)		14.83	6.28	58.2	10.36	47.80	0.69	0.29	0.55	0.089
P(NmCP)	t4CzIPN (6 wt.%)	22.58	2.94	57.1	13.32	43.77	0.59	0.39	0.34	0.14
P(mCP)		18.49	3.30	57.4	13.61	43.79	0.73	0.13	0.41	0.12

[a] Prompt lifetime. [b] Delayed lifetime. [c] Total PLQY. [d] PLQY of PF [e] PLQY of DF estimated using the corresponding proportions in the transient decay curve. [f] Radiative decay rate constant of the singlet excited state. [g] Non-radiative decay rate constant for singlet excited state. [h] Intersystem crossing rate constant, [i] RISC rate constant.

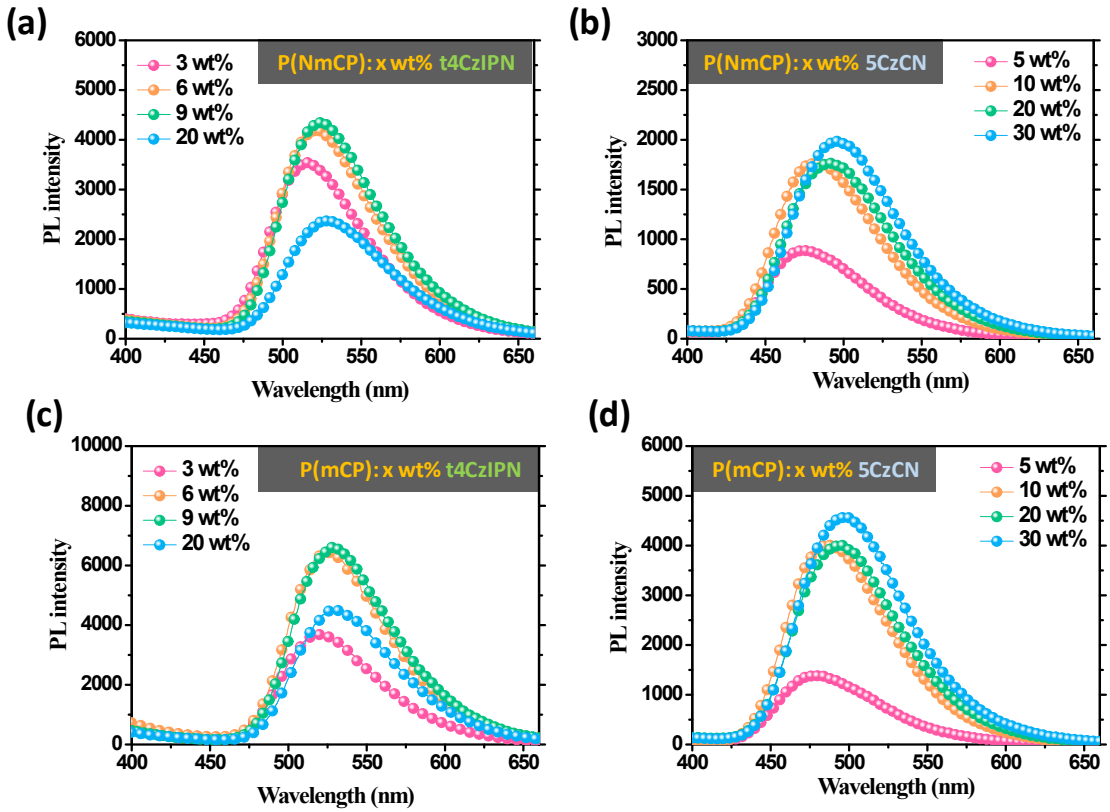

Figure S4. PL spectra of blend films according to composition change of TADF dopant. (a, b) **P(NmCP)** host, (c, d) **P(mCP)** host.

We used green (t4CzIPN) and blue dopants (5CzCN) to measure the PL intensity in the blend film state to optimize the concentration of the dopant. By changing the dopant concentration, energy transfer from the host to the dopant occurs effectively, and in general, the dopant concentration was selected when the emission intensity of the dopant reaches the maximum value. As a result of this experiment, the optimized concentrations of t4CzIPN and 5CzCN were selected to be 6 and 20 wt%, respectively.

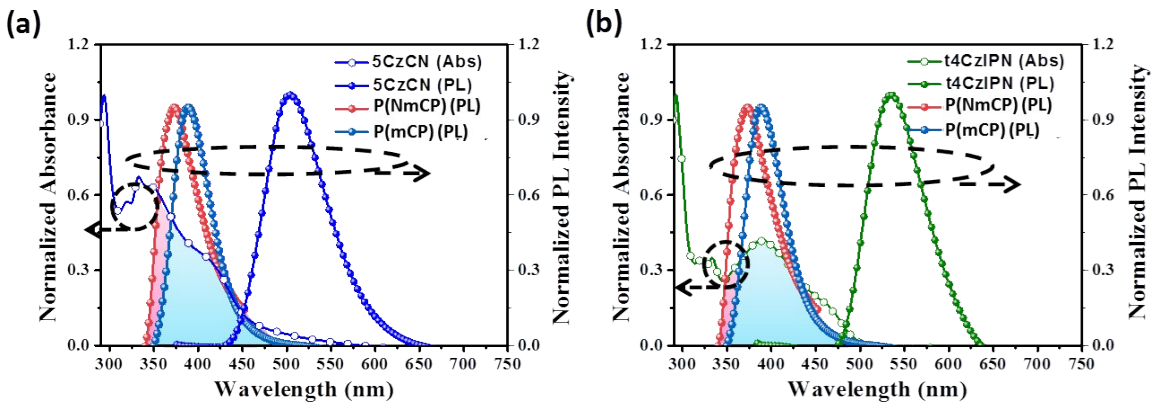

Figure S5. PL spectra of the polymeric hosts. Absorption and PL spectra of the TADF emitter.

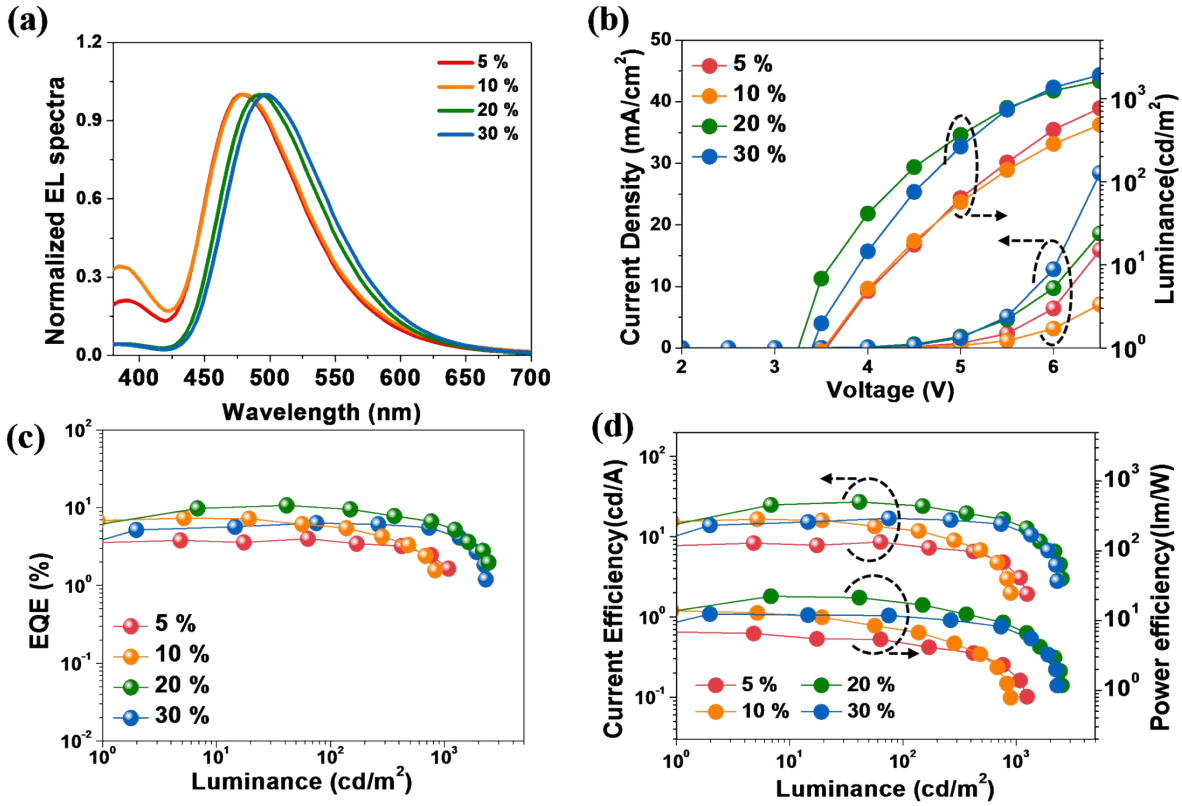

Figure S6. (a) EL spectra of the sky-blue emitting devices at a luminance of 1000 cd/m^2 (b) current density-voltage-luminance (*J*-*V*-*L*) curves, (c) EQE vs luminance (EQE-*L*) curves, and (d) current efficiency – Luminance – power efficiency (CE-*L*-PE) curves for solution-processed TADF-OLED devices with various 5CzCN concentration with **P(NmCP)** as the host.

Table S2. Performances of solution-processed TADF-OLED devices with various 5CzCN concentration with **P(NmCP)** as the host.

Host	Emitter Conc. (wt.%)	V_{on} [a] (V)	CE_{max} [b] (cd/A)	PE_{max} [c] (lm/W)	L_{max} [d] (cd/m²)	EQE_{max} [e] (%) Maximum	500 cd/m²	1000 cd/m²	CIE (x,y) [f]
P(NmCP)	5	3.5	8.58	6.89	1250	3.99	2.98	1.80	(0.18, 0.30)
	10	3.5	16.48	13.89	893	7.34	3.30	-	(0.19, 0.31)
	20	3.10	27.13	22.30	2533	10.70	7.28	5.77	(0.21, 0.41)
	30	3.2	16.93	12.43	2312	6.35	5.74	4.70	(0.22, 0.44)

[a] Turn-on voltage of 1 cd/m^2. [b] Maximum current efficiency [c] Maximum power efficiency [d] Maximum luminance. [e] Maximum external quantum efficiency at maximum/500/1000cd/m^2. [f] Commission Internationale de L'Eclairage coordinates at 1000 cd m^{-2}. Device configuration : ITO/PEDOT:PSS (40 nm) / PX2Cz (20 nm)/ x wt.% 5CzCN : P(NmCP) (15 nm) / TPBi (40 nm) / LiF (1 nm) / Al (100 nm)

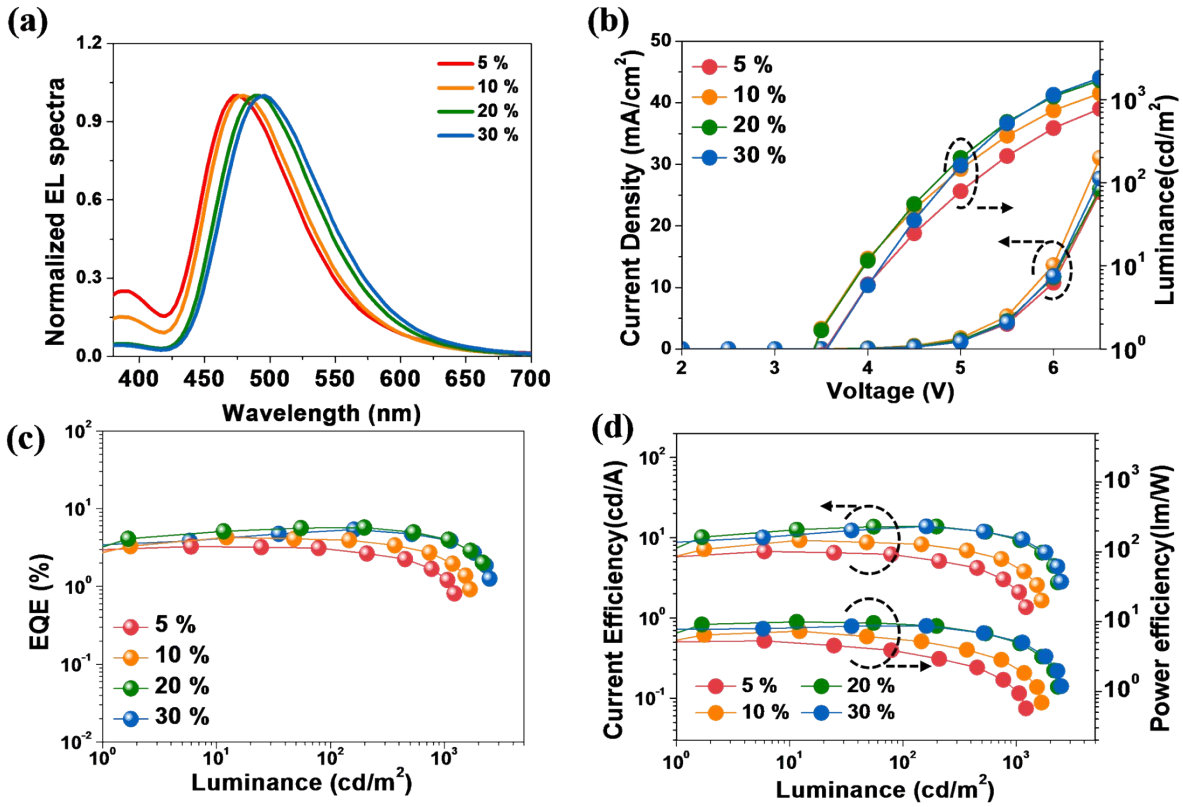

Figure S7. (a) EL spectra of the sky-blue emitting devices at a luminance of 1000 cd/m^2 (b) current density-voltage-luminance (*J-V-L*) curves, (c) EQE vs luminance (EQE-*L*) curves, and (d) current efficiency – Luminance – power efficiency (CE-*L*-PE) curves for solution-processed TADF-OLED devices with various 5CzCN concentration with **P(mCP)** as the host.

Table S3. Performances of solution-processed TADF-OLED devices with various 5CzCN concentration with **P(mCP)** as the host.

Host	Emitter Conc. (wt.%)	V_{on} [a] (V)	CE_{max} [b] (cd/A)	PE_{max} [c] (lm/W)	L_{max} [d] (cd/m²)	EQE_{max} [e] (%) Maximum	500 cd/m²	1000 cd/m²	CIE (x,y) [f]
P(mCP)	5	3.5	6.75	5.30	1223	3.26	2.20	1.26	(0.18, 0.27)
	10	3.3	9.28	7.29	1678	4.28	3.08	2.20	(0.18, 0.30)
	20	3.3	13.80	9.91	2335	5.73	5.14	4.07	(0.20, 0.38)
	30	3.5	13.81	8.68	2494	5.39	4.71	4.00	(0.21, 0.42)

[a] Turn-on voltage of 1 cd/m^2. [b] Maximum current efficiency [c] Maximum power efficiency [d] Maximum luminance. [e] Maximum external quantum efficiency at maximum/500/1000cd/m^2. [f] Commission Internationale de L'Eclairage coordinates at 1000 cd m^{-2}. Device configuration : ITO/PEDOT:PSS (40 nm) / PX2Cz (20 nm)/ x wt.% 5CzCN : P(NmCP) (15 nm) / TPBi (40 nm) / LiF (1 nm) / Al (100 nm)

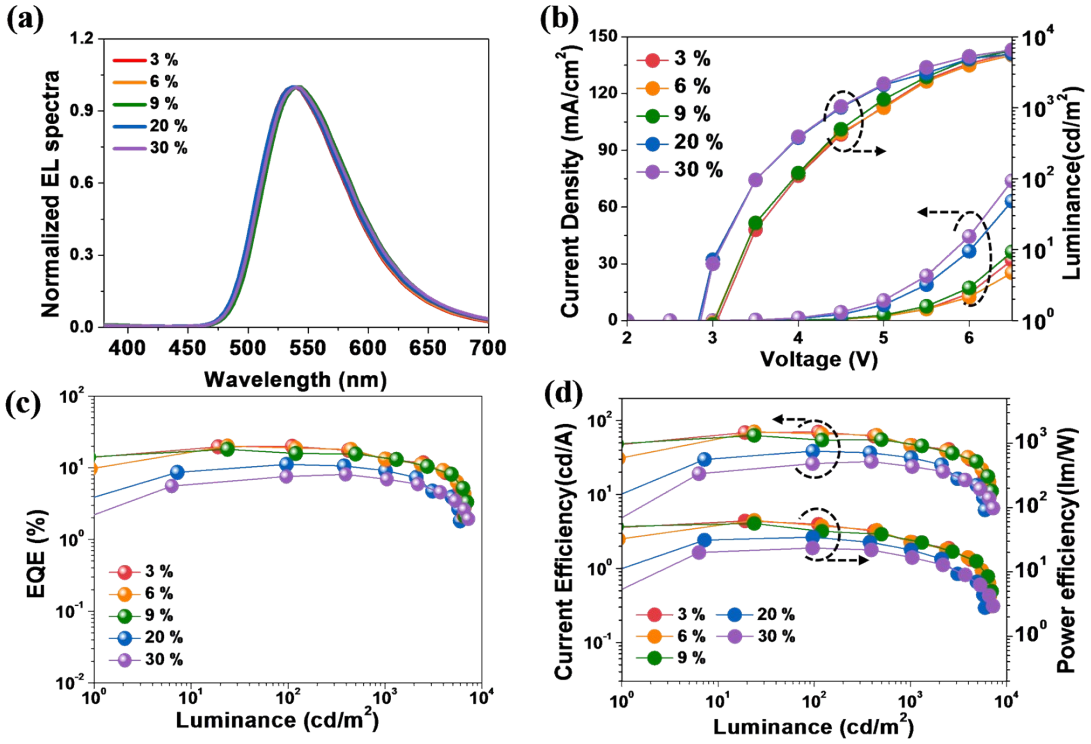

Figure S8. (a) EL spectra of the green emitting devices at a luminance of 1000 cd/m^2 (b) current density-voltage-luminance (*J-V-L*) curves, (c) EQE vs luminance (EQE-*L*) curves, and (d) current efficiency – Luminance – power efficiency (CE-*L*-PE) curves for solution-processed TADF-OLED devices with various t4CzIPN concentration with **P(NmCP)** as the host

Table S4. Performances of solution-processed TADF-OLED devices with various t4CzIPN concentration with **P(NmCP)** as the host.

Host	Emitter Conc. (wt.%)	V_{on} [a] (V)	CE_{max} [b] (cd/A)	PE_{max} [c] (lm/W)	L_{max} [d] (cd/m^2)	EQE_{max} [e] (%)			CIE (x,y) [f]
						Maximum	500 cd/m^2	1000 cd/m^2	
	3	3.0	70.09	61.85	6740	19.92	16.68	13.15	(0.36, 0.59)
	6	3.0	70.36	63.15	6643	20.07	17.41	13.15	(0.36, 0.59)
P(NmCP)	9	3.0	62.99	56.54	6985	18.08	15.99	13.73	(0.38, 0.58)
	20	2.9	38.56	34.61	5958	11.15	10.21	9.19	(0.37,0.59)
	30	2.9	27.88	23.48	7236	8.07	7.89	6.90	(0.38,0.59)

[a] Turn-on voltage of 1 cd/m^2. [b] Maximum current efficiency [c] Maximum power efficiency [d] Maximum luminance. [e] Maximum external quantum efficiency at maximum/500/1000cd/m^2. [f] Commission Internationale de L'Eclairage coordinates at 1000 cd m^{-2}. Device configuration : ITO/PEDOT:PSS (40 nm) / PX2Cz (20 nm)/ x wt.% t4CzIPN : P(NmCP) (15 nm) / TPBi (40 nm) / LiF (1 nm) / Al (100 nm)

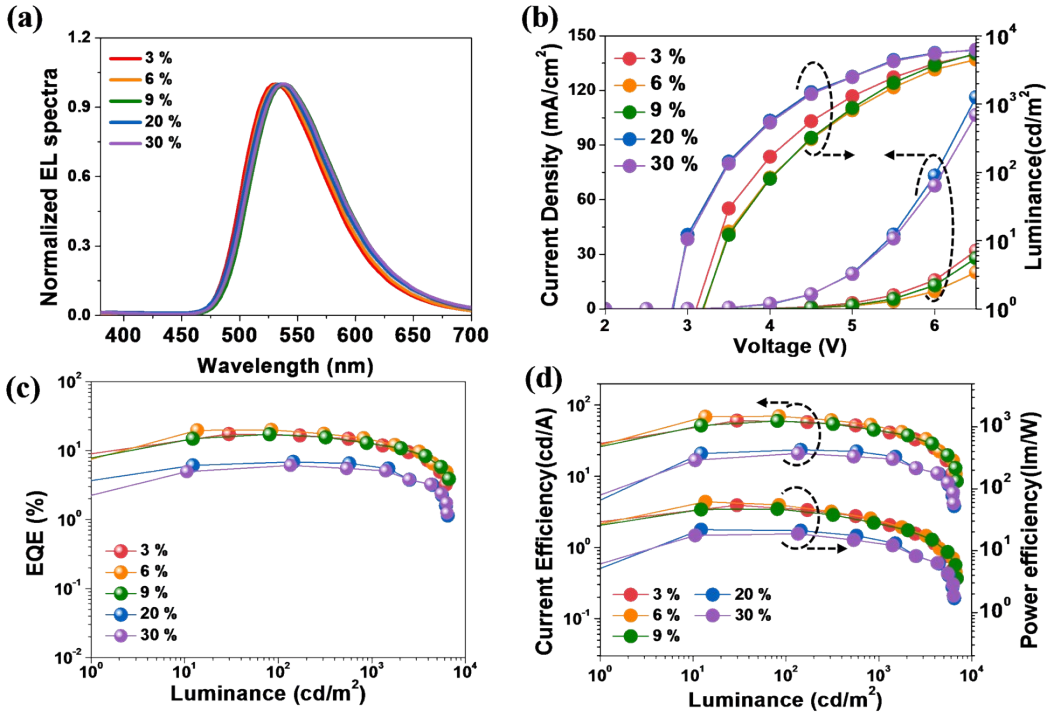

Figure S9. (a) EL spectra of the green emitting devices at a luminance of 1000 cd/m^2 (b) current density-voltage-luminance (*J*-*V*-*L*) curves, (c) EQE vs luminance (EQE-*L*) curves, and (d) current efficiency – Luminance – power efficiency (CE-*L*-PE) curves for solution-processed TADF-OLED devices with various t4CzIPN concentration with **P(mCP)** as the host.

Table S5. Performances of solution-processed TADF-OLED devices with various t4CzIPN concentration with **P(mCP)** as the host.

Host	Emitter Conc. (wt.%)	V_{on} [a] (V)	CE_{max} [b] (cd/A)	PE_{max} [c] (lm/W)	L_{max} [d] (cd/m²)	EQE_{max} [e] (%)			CIE (x,y) [f]
						Maximum	500 cd/m²	1000 cd/m²	
P(mCP)	3	3.0	60.55	54.35	6179	17.33	15.13	12.70	(0.34, 0.60)
	6	3.0	69.88	61.80	6720	19.66	16.09	14.02	(0.35, 0.60)
	9	3.0	59.97	47.10	6914	17.18	14.02	12.70	(0.37, 0.59)
	20	2.8	23.52	21.91	6478	6.84	6.57	5.89	(0.36,0.59)
	30	2.8	20.93	18.78	6366	6.09	5.50	5.22	(0.37,0.59)

[a] Turn-on voltage of 1 cd/m^2. [b] Maximum current efficiency [c] Maximum power efficiency [d] Maximum luminance. [e] Maximum external quantum efficiency at maximum/500/1000cd/m^2. [f] Commission Internationale de L'Eclairage coordinates at 1000 cd m^{-2}. Device configuration : ITO/PEDOT:PSS (40 nm) / PX2Cz (20 nm)/ x wt.% t4CzIPN: P(NmCP) (15 nm) / TPBi (40 nm) / LiF (1 nm) / Al (100 nm)

Reference

1 M. Godumala, J. Hwang, H. Kang, J.-E. Jeong, A. Harit, M. J. Cho, H. Y. Woo, S. Park, D. H. Choi, *ACS Appl. Mater. Interfaces*, 2020, **23**, 35300-35310

2 J. H. Lee, C. H. Jeong, M. Godumala, C. Y. Kim, H. J. Kim, J. H. Hwang, Y. W. Kim, D. H. Choi, M. J. Cho and D. H. Choi, *J. Mater. Chem. C*, 2020, **8**, 4572-4579.